Static structure factor of two-dimensional liquid 3He adsorbed on graphite

Ahmad Sultan, Matthias Meschke, Hans J. Lauter, Henri Godfrin

Journal of Low Temperature Physics manuscript No.
(will be inserted by the editor)

A. Sultan · M. Meschke · H.-J. Lauter · H. Godfrin

Static structure factor of two-dimensional liquid ^{3}He adsorbed on graphite

Received: date / Accepted: date

Abstract Liquid ^{3}He is a model system for strongly correlated Fermi liquids. For this reason, many X-ray and neutron scattering experiments have been performed to understand the structure and dynamics of this quantum fluid. We have recently shown that two-dimensional liquid ^{3}He sustains long-lived zero-sound excitations at large wave-vectors (Nature **483**, 576, 2012). Here we show that its static structure factor can be obtained with reasonable accuracy by integrating the experimental S(Q,ω) over a suitable energy range. A good agreement is found between the static structure factor deduced from the experiment and theoretical models: Quantum Monte Carlo simulations and Dynamical Many Body Theory (DMBT). At high wave-vectors, the experimental values are underestimated because of the limited accessible phase space; nevertheless, even at atomic wave-vectors a semi-quantitative agreement is observed with the theoretical predictions.

Keywords Helium three · Fermi liquids · Two-dimensional quantum fluids · Structure factor

PACS 67.10.Hk · 05.30.Fk · 67.10.Db

A. Sultan and H. Godfrin
Institut Néel, CNRS et Université Joseph Fourier, BP 166, 38042 Grenoble cedex 9, France
E-mail: henri.godfrin@grenoble.cnrs.fr

M. Meschke
Low Temperature Laboratory, Aalto University, PO Box 15100, 0076 Aalto, Finland

H.-J. Lauter
Institut Laue-Langevin, BP 156, 38042 Grenoble cedex 9, France
Oak Ridge National Laboratory, PO Box 2008, Oak Ridge TN 37831-6475, USA

1 Introduction

The static structure factor S(Q) is a quantity experimentally accessible by neutron or X-ray diffraction. It depends essentially on the atomic radial distribution function and can be determined by calculating the Fourier transform of the latter. The static structure factor is given by the expression:

$$S(Q) = \frac{1}{N}\langle \rho_Q \rho_{-\mathbf{Q}} \rangle \tag{1}$$

where N and ρ_Q are respectively the number of atoms and the Fourier transform of the microscopic density $\rho(\mathbf{r})$.

S(Q) is usually measured by neutron or X-ray diffraction, but this simple technique cannot be used in practice in the case of two-dimensional ^{3}He atoms adsorbed on graphite: the very strong background due to the solid substrate would dominate the signal from the ^{3}He atoms by several orders of magnitude. Using *neutron inelastic scattering*, however, it is possible to separate the contribution of the helium from that of the substrate. We present in this manuscript a first attempt to determine the static structure factor of a submonolayer liquid ^{3}He film. The latter is adsorbed on a graphite substrate preplated with one solid layer of ^{4}He. The experimental results for S(Q) were obtained by integrating the data of S(Q,ω) [1] over a carefully determined (wave-vector dependent) energy range, as described below.

Our study of the two-dimensional Fermi liquid ^{3}He was motivated by several points. Two-dimensional ^{3}He has a similar topology as bulk ^{3}He. Indeed, in the case of the 2D system, ^{3}He atoms populate the energy levels giving rise to a Fermi disk in **k**-space, while in 3D, we obtain a Fermi sphere. However, the absence of a critical point in two-dimensional ^{3}He allows the exploration of a larger density range, going from zero (Fermi gas) to very high ones, until the system solidifies. We can therefore study Fermi liquids with an effective mass varying from $m^* =$ m to much higher values than those found in bulk ^{3}He [2–6]. For a 2D layer of density $\rho = 4.7 \pm 0.2\, atoms/nm^2$ the effective mass is about four times the bare mass of a ^{3}He atom, this can be obtained in a bulk system by applying a pressure of 1MPa.

Present many-body theories have reached a degree of accuracy which enables them to provide quantitative predictions for the static structure factor of such a system. Confronting the experimental result with these theoretical predictions is therefore of interest. In addition, a test of the accuracy of the density determined in our previous works by indirect means, can be obtained from a comparison with the theory, using the shift of the maximum of S(Q) with density.

We have shown previously a good agreement between the excitation spectrum of the two-dimensional Fermi liquid ^{3}He calculated by DMBT and the values of S(Q,ω) obtained experimentally [1]. DMBT adopts the view that the physical mechanisms which determine the short-wavelength spectrum are the same in ^{3}He and ^{4}He. Based on this assumption, the DMBT has been developed by generalizing the bosonic dynamic many-body theory [7–9] which describes with good accuracy the excitation spectrum of ^{4}He. The novelty in the fermionic version of DMBT [10] is that it takes into account the pair correlations. The DMBT for two-dimensional systems predicts correctly all the excitations observed in the

measurement of the inelastic spectrum [1]; however, an accurate quantitative fit of the experimental data with the theory is still not possible, due to higher order effects. However, these corrections are expected to affect only moderately the static structure factor. DMBT direct calculations of S(Q) were performed by the Linz group, providing us with a prediction for S(Q) at a density close to that of our experimental system. Further details about this theory are given in reference [11].

We also compare our experimental results to diffusion Monte Carlo calculations performed for similar densities [12]. The theory allows the derivation of effective interactions. Assuming that the dynamic susceptibility is given by the Random Phase approximation (equation 2), the static structure factor can be deduced from dynamic response functions:

$$\chi(Q,\omega) = \frac{\chi_0(Q,\omega)}{1-\tilde{V}(Q)\chi_0(Q,\omega)} \tag{2}$$

$$S(Q) = -\int_0^\infty \frac{d(\hbar\omega)}{\pi} Im\big[\chi(Q,\omega)\big] \tag{3}$$

where $\chi_0(Q,\omega)$ is the generalized susceptibility of the Fermi gas. $\tilde{V}(Q)$ is the Fourier transform of the potential. The expression 3 is obtained by applying the m_0 sum rule [13]:

$$S(Q) = \int d\omega\, S(Q,\omega) \tag{4}$$

2 Two-dimensional Fermi liquid

Because of its perfectly spherical Fermi surface, its relatively simple Hamiltonian and its very high purity, liquid ^{3}He is a perfect candidate for studying highly correlated Fermions. Its properties are described by Landau's Fermi liquid theory, which is valid at low momentum transfer and low temperatures. The effective mass of quasi-particles (m^*), specific heat (C_V) and magnetic susceptibility (χ_0) of a Fermi liquid can be deduced from the bare mass of ^{3}He, the specific heat (C_V^g) and the magnetic susceptibility (χ^g) of a Fermi gas, with renormalization factors, expressed in terms of the Landau parameters which parametrize the interactions. The formulae applicable in two dimensions [14] are similar to their 3D analogues:

$$m^* = m(1+1/2\cdot F_1^s) \tag{5}$$

$$C_V = \frac{m^*}{m} C_V^g = (1+1/2\cdot F_1^s)\, C_V^g \tag{6}$$

$$\chi_0 = (1+1/2\cdot F_1^s)\Big(\frac{1}{1+F_0^a}\Big)\,\chi^g \tag{7}$$

Here m is the bare mass of a ^{3}He atom, and F_1^s and F_0^a are Landau's parameters that depend on the interactions, and hence on density.

The properties of two-dimensional ^{3}He can be deduced from the expressions below, with numerical values calculated for $\rho = 4.7 \pm 0.2$ atoms/nm^2, the density investigated here.

Fig. 1 In order to smooth the potential and obtain a two-dimensional homogeneous Fermi liquid, ^{3}He is adsorbed on a graphite substrate preplated with a solid ^{4}He layer.

$$k_F = \sqrt{2\pi\rho} = 5.43 \pm 0.12\, nm^{-1} \tag{8}$$

$$E_F = \frac{\hbar^2 k_F^2}{2m} = 0.04355\,\rho = 0.204 \pm 0.009\, meV \tag{9}$$

$$T_F = \frac{E_F}{k_B} = 0.5053\,\rho = 2.37 \pm 0.10\, K \tag{10}$$

3 Sample characteristics

Experimental details have been given in previous publications [1,15,16]; for clarity, we summarize in the following the most relevant experimental parameters. We discuss in more detail the background subtraction, essential to the object of the present article, the determination of S(Q). Because of the large absorption of neutrons by ^{3}He atoms and the large background due to the substrate, the data analysis required a special treatment. We discuss in the next section the experimentally accessible region where S(Q,ω) was obtained with good accuracy.

In order to obtain a homogeneous two-dimensional liquid ^{3}He film, we used a high quality exfoliated graphite substrate (Union Carbide ZYX). The graphite substrate has been characterized by neutron diffraction experiments at the ILL[1, 15]. In order to make the adsorption potential more homogeneous for the ^{3}He atoms, we preplate the substrate with a solid layer of ^{4}He atoms as shown on figure 1. The maximum density of the first layer is 11.6 atoms/nm^2. All additional atoms introduced in the cell will populate the second layer. We introduce a volume of 28.59 cm^{3}STP (standard conditions of temperature and pressure) of ^{4}He atoms. This corresponds to a layer's density of 11.3 atoms/nm^2 (we take into account the compression due to the adsorption of atoms on the second layer). Then we introduce in the cell a volume of 11.0 cm^{3}STP, we thereby obtain a ^{3}He layer of density 4.7 $\pm$ 0.2 atoms/nm^2 (the uncertainty being due to that on the effective surface area available for adsorption). Adsorption isotherms are performed at 4.2 K, annealing of the films is done by lowering the temperature progressively from 20 K, with steps at adequate intermediate temperatures. The neutron measurements are performed at a temperature of about 50 mK.

4 Neutron set-up

Before measuring the dynamical structure factor of the two-dimensional ^{3}He sample, the signal of the bare graphite as well as that obtained with the ^{4}He solid layer

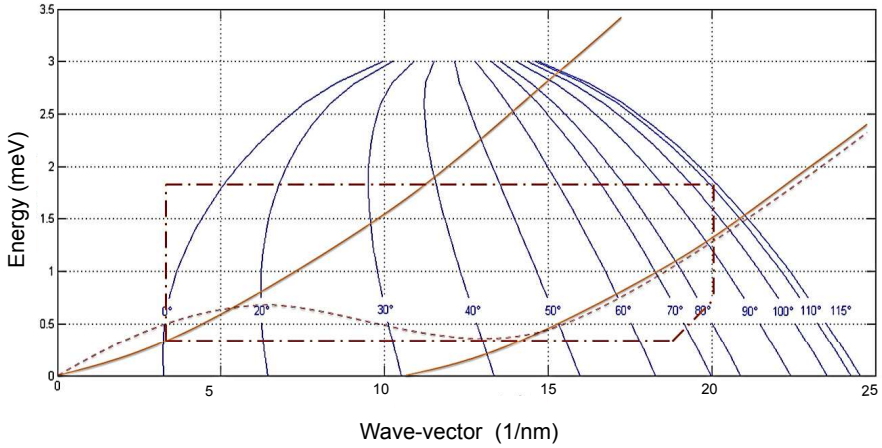

Fig. 2 Accessible phase space (Q,ω) calculated for incident neutrons of wavelength 0.512 nm. The lines labeled by different angles indicate the positions in the [Q,ω] plane covered by different detectors. Only the part corresponding to a positive energy transfer is shown on the figure. Thick solid lines indicate the limits of the particle-hole band, the dashed line the dispersion of the zero-sound mode observed in two-dimensional Fermi liquid ^{3}He [1], and the dashed frame the region were background subtraction is possible.

have been measured in detail. All the data have been taken on the IN6 time-of-flight instrument at the ILL. In this instrument, the wavelength of the incident neutrons is selected by Bragg reflection on graphite crystal monochromators. An incident beam wavelength of 0.512 nm was selected. The beam is then conditioned in short packets of monochromatic neutrons by a Fermi chopper. After interacting with the sample, the neutrons are scattered in multiple directions depending on the momentum transfer in the process of creating excitations. They are finally collected by a detector bank covering a wide angular range, from 10 ° to 115 °. The time of arrival of each neutron as well as the scattering angle are registered. From this information we obtain the double differential cross-section, and hence the dynamical structure factor of the system:

$$\begin{aligned}\frac{\partial^2\sigma}{\partial\Omega\partial t} &= \frac{dE_{|k'\rangle}}{dt}\frac{\partial^2\sigma}{\partial\Omega\partial E_{|k'\rangle}} \\ &= \frac{N\sigma}{2\pi\sqrt{E_{|k\rangle}}}\left(\frac{m}{2}\right)^{3/2}\frac{L^3}{t^4}\cdot S(Q,\omega)\end{aligned} \tag{11}$$

where $\frac{\partial^2\sigma}{\partial\Omega\partial t}$ is the double differential cross-section which yields the number of scattered neutrons per unit of time in a solid angle $d\Omega$. N is the number of scattering centers, L the distance between the sample and the detectors, t the time of arrival of neutrons, m their mass, $E_{|k\rangle}$ and $E_{|k'\rangle}$ are respectively the energy of incident and scattered neutrons.

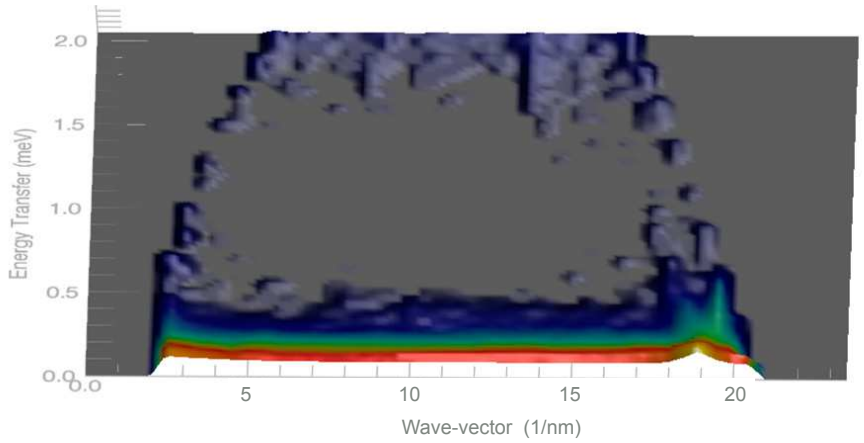

Fig. 3 Schematic representation of the dynamical structure factor of the bare graphite substrate. The intensity is represented in the third dimension in a logarithmic scale. The signal at low energies corresponds to very high intensities, but significant background is also present elsewhere, seen as spots. Measurement is possible only in the central, uniform part of the [E,Q] area, where background is comparable to the very weak ^{3}He signal.

5 Neutron measurements and background subtraction

The experimentally accessible phase space in the (Q,ω) plane is determined using the equation:

$$Q^2 = \frac{2\pi}{\lambda}\left(1 - \frac{\hbar\omega}{2E_{|k\rangle}} - \sqrt{1 - \frac{\hbar\omega}{E_{|k\rangle}}}cos(\phi)\right) \tag{12}$$

where ϕ is the angle at which the detectors are located, λ the wavelength of the incident neutrons, $\hbar\omega$ and Q are respectively the energy and momentum transfer. The lines in figure 2 represent different constant angles (i.e. detectors) in the range from 10° to 115°. In principle all the region encompassed by the lines corresponding to angles between 10° and 115° and energies from zero to that of the incident neutrons, is accessible experimentally. In practice, however, good statistics and an accurate subtraction of background is obtained in a much smaller region of the phase space (dashed frame in figure 2). This is due to the combination of several effects, which lead to the background depicted in figure 3:

1. The region at high energy transfers ($\hbar\omega > 1.8$ meV) is contaminated by frame-overlap. The effect is due to simultaneous detection of slow neutrons of a packet and fast neutrons of the following one. Exploration of S(Q,ω) of ^{3}He in this region becomes difficult.
2. At low energy transfers ($\hbar\omega < 0.3$ meV), the graphite elastic peak at Q = $19\,\mathrm{nm}^{-1}$ (Bragg peak) is very intense. Moreover, the adsorption of helium layers leads to a reduction of the finite size effects associated with the graphite powder, i.e., the scattering planes represented by the helium adsorbed layers can be seen as increasing the rather small number of graphite planes of each graphite platelet, and hence leading to a better definition of the corresponding

diffraction peak, and therefore to a reduction of the width of the graphite's elastic signal (see [17] and references therein). Subtraction of the background for such momentum transfers requires a delicate fitting procedure.

3. At high wave-vector transfers, a phonon branch is observed in the substrate spectra (see figure 3). The additional neutron counts in the background increase the statistical uncertainty in this region. However, this feature is useful to check the accuracy of background subtraction after performing corrections for neutron absorption by the ^{3}He.
4. No supplementary contributions to the background are observed when ^{4}He atoms are introduced in the cell. The background changes slightly, in particular due to interference effects mentioned before, but no new feature is observed. Indeed, because of its high density, the Bragg peak of the ^{4}He layer is located at $Q = 22.6\,\mathrm{nm}^{-1}$ and is thus outside the experimentally accessible wave-vector region.

For the reasons listed above, the dynamical structure factor $S(Q,\omega)$ of the ^{3}He layer can be determined reliably only in the region delimited by the dashed frame of figure 2. The static structure factor S(Q) is calculated here by integrating, over energies, the dynamical structure factor. The energy range where this can be done is clearly limited, but we shall see below that the important contributions to S(Q) are essentially captured.

6 Results and discussions

Figure 4 shows a cut of $S(Q,\omega)$ at the wave-vector Q = 17.5 nm^{-1}. Note that by integrating the dynamical structure factor in a range $0.3 < \hbar\omega < 1.8$ meV, a non-negligible part of the signal from the particle-hole band is not taken into account. By comparing figure 2 and 3 (see also ref [1]), it is clear that below wave-vectors on the order of 15 nm^{-1} both the particle-hole band and the collective zero-sound mode, which carry most of the spectral weight, will be correctly integrated, while above this value, part of the particle-hole band will be left out of the integration interval. Fortunately, contrarily to early RPA predictions, the particle-hole band weight at high wave-vectors is concentrated at low energies; hence the fraction lost in the integration is moderate, as can be seen from figure 4.

Despite the experimental difficulties, we were able to extract the static structure factor S(Q) from the experimental data with reasonable accuracy. In figure 5, we compare the experimental $S(Q)$ with the results of DMBT and Quantum Monte Carlo simulations. The data are essentially 'neutron counts' normalized to different experimental parameters (incident flux, spectrometer geometry, sample dimensions, etc...); they are proportional to the structure factor, but unfortunately they cannot be normalized with sufficient accuracy to infer absolute values of this magnitude. For this reason, the data expressed in arbitrary units have been normalized to agree with theory at Q = 5.5 nm^{-1}, a region where the precision of experiments is good, and where they capture all the expected inelastic contributions to S(Q).

We observe a good agreement in the region of low wave-vectors, in particular a significant shoulder is seen in the S(Q) data which corresponds well to the theoretical predictions. At $Q \approx 12$ nm^{-1} the particle hole-band leaves the frame where

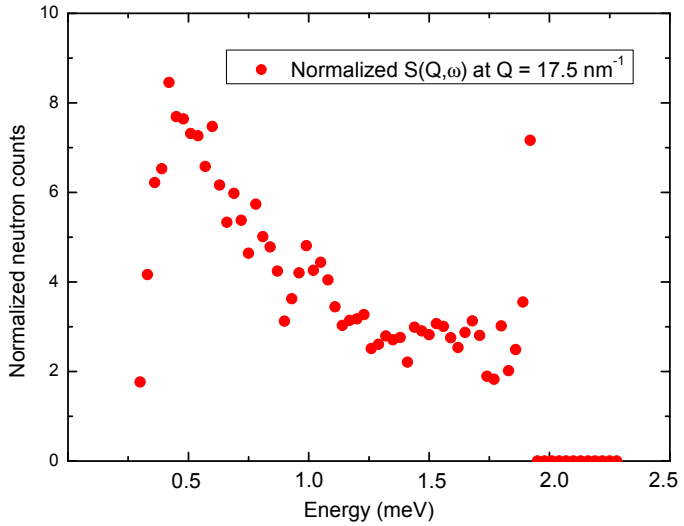

Fig. 4 Experimental S(Q,ω) for the wave-vector Q = 17.5 nm^{-1} as a function of energy. The figure shows the range where the integral over energy can be performed reliably. The large intensity measured at the highest energies is due to frame-overlap.

S(Q,ω) is integrated, and the experimental value of S(Q) starts to diverge from the theoretical curves. Nevertheless, because of the high intensity and the low energy of the roton-like minimum, a maximum of S(Q) is found. Then the signal collapses because the integration of the particle-hole band is carried over a limited region. A reasonable semi-quantitative agreement is obtained between theory and experiment. The peak in S(Q) is seen to coincide with the theoretical equivalent feature, confirming the accuracy of the determination of the layer's density. This magnitude is important, and difficult to obtain; it was determined previously by indirect means (adsorption isotherms and neutron diffraction at higher coverages on the solid phases, where Bragg peaks are seen) [1, 15]. Note that the wave-vector corresponding to the roton minimum, that of the maximum in S(Q), and 2π divided by the interparticle distance are related (but different) quantities of similar atomic dimensions, and that only an accurate many-body theory will be able to establish a quantitative relation among them [10, 13]. They also have different dependencies on density. For these reasons, comparing directly the theoretical and experimental values of S(Q) is a particularly valuable tool to infer the actual density of the liquid layer .

7 Conclusions

We presented in this article a comparison between the static structure factor of a two-dimensional Fermi liquid, a ^{3}He film adsorbed on a graphite substrate pre-

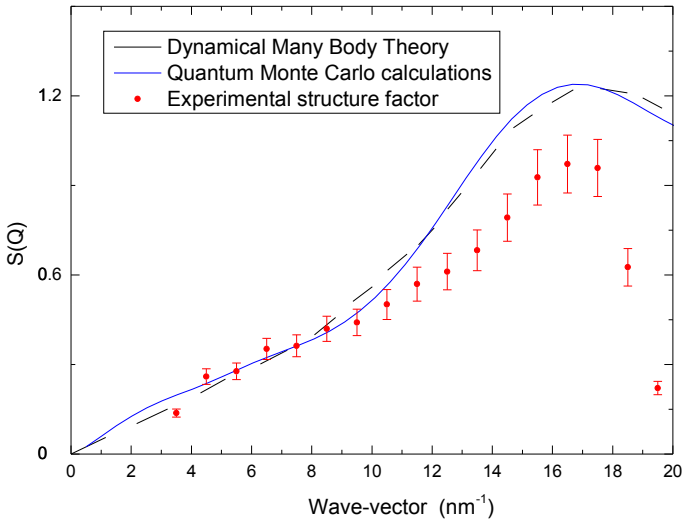

Fig. 5 S(Q) obtained experimentally compared to theoretical calculations: the Dynamical Many-Body Theory and Monte Carlo simulations. The error bars on the experimental data only reflect statistical uncertainties; the systematic deviation at large wave-vectors is due to the finite integration range, see text.

plated with a solid ^{4}He layer. The large background of such a system makes difficult the determination of S(Q) by direct methods as neutron diffraction. Using inelastic neutron scattering data measured on the instrument IN6 at the ILL, we were able to deduce the static structure factor by integrating S(Q,ω) in an energy range covering a large fraction of the inelastic contributions. The comparison with theory shows important features: at low wave-vectors a good agreement with theory is observed. A shoulder is seen as predicted by the Dynamical Many-Body Theory and Quantum Monte Carlo simulations. At high wave-vectors a maximum is obtained around Q $= 16$ nm^{-1}, value where a roton-like mode has been seen in S(Q,ω) [1], in good agreement with the theoretical calculations. This feature provides an independent check of the film density determination. Deviations from the theoretical curves observed at very high wave-vectors can be accounted for semi-quantitatively by the limited experimental energy range. The elaborated procedure used to separate the signal of the ^{3}He layer from the background turns out to be essential for extracting S(Q) with reasonable accuracy from the inelastic data.

Acknowledgements This work was supported by the EU FRP7 low-temperature infrastructure grant Microkelvin (project number 228464), the French-Austrian grant High-Q Fermions (ANR-2010-INTB-403-01 and FWF-P21264), and the Institut Laue-Langevin through the use of the neutron facility. Discussions with Ph. Nozières, H. Böhm, E. Krotscheck, M. Panholzer, J. Boronat, M. Holzmann, S. Hernandez and J. Navarro are gratefully acknowledged.

References

1. H. Godfrin, M. Meschke, H.-J. Lauter, A. Sultan, H. Böhm, E. Krotscheck and M. Panholzer, Observation of a roton collective mode in a two-dimensional Fermi liquid, Nature, 483, 576-579 (2012).
2. D.S. Greywall, Heat capacity of multilayers of ^{3}He adsorbed on graphite at low millikelvin temperatures, Phys. Rev. B 41, 1842-1862 (1990).
3. K.D. Morhard, C. Bäuerle, J. Bossy, Yu.M. Bunkov, S.N. Fisher and H. Godfrin, Two-dimensional Fermi liquid in the highly correlated regime: the second layer of ^{3}He adsorbed on graphite, Phys. Rev. B 53, 2658-2661 (1996).
4. C. Bäuerle, Yu. M. Bunkov, A.S. Chen, S.N. Fisher and H Godfrin, Ultra-low temperature magnetic properties of liquid ^{3}He films, J. of Low Temp. Phys. 110, 333-338 (1998).
5. A. Casey, H. Patel, J. Nyéki, B.P. Cowan, and J. Saunders, Strongly correlated two- dimensional fluid ^{3}He, J. of Low Temp. Phys. 113, 293-298 (1998).
6. M. Neumann, J. Nyéki, B.P. Cowan, and J. Saunders, Bilayer ^{3}He: a simple two-dimensional heavy-fermion system with quantum criticality, Science 317, 1356-1359 (2007).
7. H. W. Jackson and E. Feenberg, Energy Spectrum of Elementary Excitations in Helium II, Rev. Mod. Phys. 34, 686 (1962)
8. E. Feenberg, Theory of Quantum Fluids, Academic, New York, (1969)
9. C. E. Campbell and E. Krotscheck, Dynamic many-body theory: Pair fluctuations in bulk ^{4}He, Phys. Rev. B 80, 174501 (2009)
10. H.M. Böhm, R. Holler, E. Krotscheck and M. Panholzer, Dynamic many-body theory: Dynamics of Strongly Correlated Fermi Fluids, Phys. Rev. B 82, 224505 (2010).
11. R. Hobbinger, R. Holler, E. Krotscheck and M. Panholzer, Multi-pair and exchange effects in the dynamic structure of two-dimensional ^{3}He, J. of Low Temp. Phys. (this issue)
12. J. Boronat, J. Casulleras, V. Grau, E. Krotscheck and J. Springer, Effective mass of two-dimensional ^{3}He, Phys. Rev. Lett. 91, 085302 (2003)
13. H.R. Glyde, Excitations in Liquid and Solid Helium, Clarendon Press, Oxford (1994).
14. A.H. Castro Neto and E. Fradkin, Bosonization of Fermi liquids, Phys. Rev. B 49, 16 (1994).
15. A. Sultan, H. Godfrin, M. Meschke, H-J. Lauter, H. Schober, H. Böhm, R. Holler, E. Krotscheck and M. Panholzer, Two-dimensional Fermi liquids sustain surprising roton-like plasmons beyond the particle-hole band, Journal of Physics: Conference Series 340, 012078 (2012).
16. H. Godfrin, M. Meschke, H.-J. Lauter, H.M. Böhm, E. Krotscheck, M. Panholzer, Observation of Zero-Sound at Atomic Wave-Vectors in a Monolayer of Liquid ^{3}He, J. of Low Temp. Phys. 158, 147-154 (2010).
17. H. Godfrin and H.J. Lauter, Progress in Low Temp. Physics, Vol.XIV, Chapter 4, p.213-320, ed. W.P. Halperin, Elsevier Science B.V., Amsterdam (1995).